

Magnetic moments in as-deposited and annealed Ni layers on Fe(001): An x-ray-dichroism study

Jan Vogel* and Maurizio Sacchi

Laboratoire pour l'Utilisation du Rayonnement Électromagnétique, Bâtiment 209D, Centre Universitaire Paris-Sud, 91405 Orsay, France

(Received 28 August 1995; revised manuscript received 12 October 1995)

We have performed linear and circular x-ray-dichroism measurements at the $L_{2,3}$ edges of Ni in as-deposited and annealed layers on an Fe(001) substrate. The linear dichroism results suggest that the magnetic dipole term $\langle T \rangle$ is small in these Ni layers. Upon annealing, the intermixing of Ni and Fe causes the Ni orbital moment to increase to twice the value for bulk fcc Ni. The possible origins of this increase are discussed. Fundamental importance is attributed to the higher localization of the Ni $3d$ states, due to the "impurity" nature intrinsic to Ni atoms diluted in Fe.

I. INTRODUCTION

Magnetic systems containing two or more $3d$ transition metals (TM), both in the form of alloys and of multilayers, are widely investigated. Most of the multilayer systems studied contain Cr or Cu layers, which can cause antiferromagnetic coupling between subsequent ferromagnetic layers (usually Fe or Co) and thus can give rise to giant magnetoresistance.¹ The combination of Ni and Fe, discussed in this paper, is not often encountered in multilayers. In alloys, however, their use is widespread, both in combination with other elements (like in FeNiB) and in binary alloys of the so-called Invar type. Another interest for this system came up when it was found that layers of Ni deposited on single crystal Fe substrates feature epitaxial growth for low coverages (≤ 4 ML).²⁻⁴ This means that Ni can be stabilized in the bcc structure, which does not exist in the bulk. Regarding the magnetic properties of bcc Ni, calculations have been done both for the bulk structure⁵ and for 1 and 2 ML of Ni epitaxially grown on Fe(100) (Ref. 6). Recently, we presented an x-ray magnetic circular dichroism (XMCD) study on these epitaxially grown layers.⁷ XMCD, the difference in absorption of a magnetic material for left and right circularly polarized x rays, is by now an established technique, giving direct information about local magnetic moments. In addition, the absorption spectra also give information about the unoccupied density of states, in an element and symmetry selective way. In this paper, we want to extend the previously published results for epitaxial layers to thicker ones (up to 15 ML), and investigate the change in the Ni magnetic moments upon alloying the Ni/Fe system. When annealing, the Ni and Fe intermix, causing a gradual replacement of Ni by Fe nearest neighbors, accompanied by a change in structure for the thick layers (from polycrystalline fcc to crystalline bcc). This leads to a strong enhancement of the Ni orbital moment (a factor 2 with respect to bulk fcc Ni) and we discuss the possible origins of this enhancement, based on our observations. In relation to the bcc epitaxial layers, we also present some linear dichroism measurements that implement our previous XMCD data.

II. EXPERIMENTAL DETAILS

The substrate we used was an Fe(100) single crystal of $9 \times 5 \times 1$ mm with the [010] axis in the length direction of

the sample. The crystal was mounted on a horseshoe magnet and introduced into an ultra high vacuum chamber (base pressure 1×10^{-10} mbar). There it was cleaned by many cycles of ion bombardment and subsequent annealing at 700 °C, until contaminants (mainly N and S) were no longer detectable with Auger electron spectroscopy (AES). Annealing was performed by electron bombardment on the back side of the crystal, while the temperature was monitored using the chromel-alumel thermocouples with which the sample was clamped onto the horseshoe magnet. The magnetic quality of the crystal was checked using the magneto-optical Kerr effect (MOKE). From *ex situ* measurements the intensity of the field was estimated to be about 100 G per ampere of current through the magnet wires. It appeared that the crystal, magnetized along the [010] axis, showed 100% remanence at zero field and a coercive field of 80 Oe. Before each evaporation of Ni, the substrate was cleaned and annealed until the correct square low energy electron diffraction (LEED) pattern was observed. The cleanliness of the surface was checked again with AES. For the Auger spectra we used a Perkin-Elmer single pass cylindrical analyzer with a coaxial electron gun.

The Ni layers were evaporated from high purity ($>99.99\%$) rods using electron bombardment. The evaporation rate was measured with a quartz crystal balance and the thickness of the deposited Ni layer was also checked by comparing the intensities of the LVV and MVV Auger lines with those of the Fe substrate. We estimate the accuracy of this procedure to be about 20%. The definition of 1 ML of Ni is with respect to the Fe bulk bcc distance (1 ML ~ 1.44 Å). During evaporation the pressure was kept below 1×10^{-9} mbar. We carefully examined the LEED for all the layers and noticed that for Ni thicknesses up to 4–5 ML there is no change with respect to the clean Fe(100) pattern while for ~ 10 ML no clear pattern is visible anymore. This is in agreement with earlier observations.²⁻⁴ During Ni evaporation the Fe substrate was kept at RT or at least not intentionally heated. The maximum reading on the thermocouple during Ni depositions corresponded to about 50 °C. Comparing the Auger spectra for the as-deposited layers with those taken after a thermal cycle evidenced the occurrence of interdiffusion already below 300 °C.

X-ray absorption spectroscopy (XAS) measurements at the Ni $L_{2,3}$ absorption edges were performed at beamline

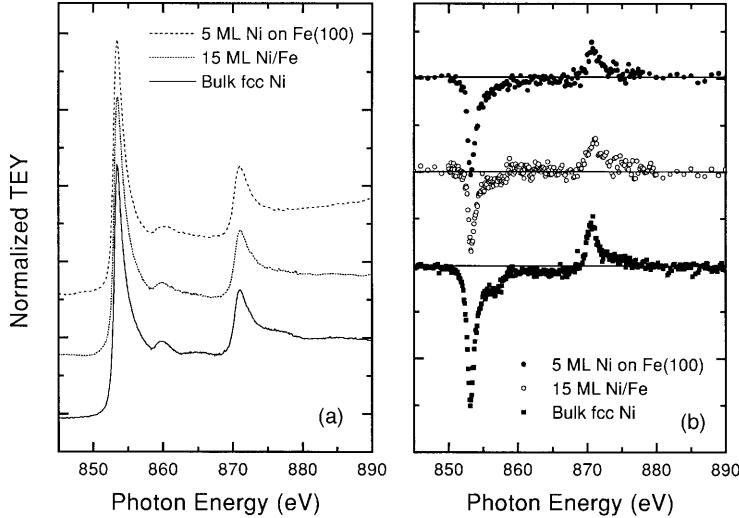


FIG. 1. (a) Total absorption spectra (sum of normalized spectra for two magnetization directions) for 5 ML and 15 ML of Ni on Fe, and bulk fcc Ni. (b) XMCD for the spectra of (a).

SA22 of the storage ring SuperACO in the laboratory LURE, Orsay, France. This line is equipped with a double crystal monochromator with natural Be(10 $\bar{1}0$) crystals which give a resolution of about 0.3 eV at the Ni L_3 edge. To measure circular x-ray dichroism, we used high precision vertical slits to select the portion of the light coming from the bending magnet 1 mrad below the plane of the ring. The light is elliptically polarized with negative helicity and the degree of circular polarization ξ_2 is about 0.9. Monochromatizing at ~ 850 eV with Beryl crystals implies two Bragg reflections close to 67° reducing ξ_2 to about 0.55 at the sample position.⁸ For the linear dichroism measurements, the in-plane light was used, having a degree of linear polarization close to 1. The absorption spectra were all measured in total electron yield (TEY) using a channeltron. The circular dichroism spectra were collected with the light in 15° grazing incidence. In this configuration one has to be aware of saturation effects,^{9,10} which might influence the spectra for the thicker layers. The data were all collected at room temperature with the Fe crystal remanently magnetized after a current pulse of about 5 A through the wires around the horse-shoe magnet. The relative orientation between the helicity of the light and the magnetization in the Fe(100) was changed simply by reversing the direction of the current through the magnet wires. Linear dichroism spectra were measured at normal incidence and at 15° grazing incidence, using p -polarized light.

III. RESULTS

A. As-deposited layers

First, let us briefly recall the sum rules for x-ray absorption as deduced by Thole *et al.*,^{11,12} applied on the $L_{2,3}$ edges of the $3d$ TM. We define the total integrated intensity of the $2p \rightarrow 3d$ transitions in the unpolarized spectrum as μ_{tot} and the integrated L_3 and L_2 intensities of the difference curve of the two spectra, taken with opposite helicities of the light, as A_3 and A_2 , respectively. For the expectation value of the orbital moment of the d shell, $\langle L_z \rangle$, in the direction of the propagation vector of the light we then get $\langle L_z \rangle = 2(A_3 + A_2)(n/\mu_{\text{tot}})$ and for the spin moment $\langle S_z \rangle = 3/2(A_3 - 2A_2)(n/\mu_{\text{tot}}) - (7/2)\langle T_z \rangle$, where n is the number of holes

in the $3d$ band and $\langle T_z \rangle$ is the expectation value of the magnetic dipole operator. Though the validity of the sum rule for the orbital moment has been well established theoretically,^{11,13} the sum rule for the spin is controversial. According to Wu *et al.*,¹³ it can give large errors even for bulk Ni, though for our measurements⁹ it gave results in good agreement with theory and with other experiments, like it was found recently also for bulk Fe and Co.¹⁴ For thin surface layers, however, the neglect of the $\langle T_z \rangle$ term might not be valid. $\langle T_z \rangle$ contains two contributions, one due to the anisotropy in the spin field which is caused by crystal field effects on the spatial distribution of the electrons, the other due to spin-orbit-coupling.¹² The first contribution is zero for a bulk cubic system, but can be important in reduced symmetry, as is the case for a surface layer.^{15,16} This contribution to $\langle T_z \rangle$ is proportional¹⁷ to $Q_{zz} * S_z$, where $\langle Q_{zz} \rangle$ is proportional to the linear dichroism.¹⁸

To estimate the importance of the $\langle T_z \rangle$ term, we have performed measurements on as deposited (1 to 3 ML) and annealed Ni layers on Fe(001) using linearly polarized photons, with the electric vector oriented parallel to the surface and 15° off the normal to the surface. Linear dichroism was observed in none of the cases, within a noise level that varied from 1 to 5% according to the specific sample. We therefore conclude that $\langle Q_{zz} \rangle$ is very small. This agrees with recent results of Guo *et al.*,¹⁹ who predicted that the linear dichroism at the Fe and Co $L_{2,3}$ edges in Fe/Co multilayers should be small. It also indicates that, at least for our samples, the contribution of crystal field effects to $\langle T_z \rangle$ is small. Also the second contribution, due to spin-orbit coupling, is expected to be small for TM due to quenching by the crystal field. This second contribution is the only one playing a role in bulk Ni, where neglecting $\langle T_z \rangle$ resulted in an accurate value for $\langle S_z \rangle$ (Refs. 9, 12, and 14).

In the assumption of a negligible $\langle T_z \rangle$, the application of the sum rule for the spin is considerably simplified. The procedure we used to apply the sum rules has been described extensively in a previous paper⁷ and the results for thin (≤ 4 ML), epitaxially grown layers have been treated there. In Fig. 1(a), the total absorption at the Ni $L_{2,3}$ edges for 5 and 15 ML of Ni on Fe(001) and bulk fcc Ni are reported, while in Fig. 1(b) the corresponding circular dichroism curves are

TABLE I. Values for orbital, spin, and total moments for as-deposited and annealed Ni layers on Fe(001). The values are obtained using sum rules on our circular dichroism data. The values for fcc Ni metal are reported for comparison.

	$\langle L_z \rangle$ (μ_B)	$\langle S_z \rangle$ (μ_B)	Total moment (μ_B)
15 ML (as dep.)	0.01 ± 0.03	0.15 ± 0.04	0.31 ± 0.10
ann. 3 min at 300 °C	0.05	0.25	0.55
5 ML (as dep.)	0.05	0.17	0.39
ann. 30 sec. at 300 °C	0.09	0.27	0.63
1 ML (as dep.)	0.05	0.14	0.33
ann. 1 min. at 400 °C ("Ni impurity")	0.11	0.26	0.63
fcc Ni	0.06	0.27	0.60

shown. To get the total absorption, the spectra for the two directions of magnetization were normalized before the L_3 and after the L_2 edge, and then summed. The total absorption for the 15 ML coverage looks more like the Ni metal spectrum than for the thinner coverages, indicating that the structure for these thick layers is getting closer to fcc. The magnetic moments extracted from the spectra using the sum rules are reported in Table I. Also the value for an epitaxial layer from Ref. 7 is given. The values are remarkably similar for all the as-deposited layers. Though the probing depth of the TEY is known to be rather short (about 20 Å for Ni) the contribution from the surface is relatively small for the thick layer. A possible breakdown of the sum rules at the surface can therefore not explain the small size of the magnetic moments in the thickest layer. However, it could be induced by the apparent polycrystallinity of the Ni, which may cause an incomplete alignment of the magnetic moments to the ones of the substrate, since all the measurements were done with the substrate in remanent magnetization.

B. Annealed layers

Changes upon annealing the Ni/Fe layers were monitored by LEED and by Auger measurements on the MVV lines of Fe and Ni. In the as deposited 15 ML sample, for example, no LEED pattern was visible (only very broad spots on a high background) and the Auger spectrum presented only the Ni contribution, a situation that did not change after flashing the sample up to 300 °C. After annealing for 30 seconds at 300 °C, the spots were still very broad, but a square pattern became visible. In the Auger spectrum, the Fe MVV line appeared (with a Ni/Fe MVV ratio of about 5). After a second annealing (for another 150 sec) at 300 °C, the Ni/Fe MVV ratio was about 0.5, the LEED spots were much narrower and showed the same pattern as for the clean Fe. The decrease in the Ni/Fe intensity ratio clearly evidences a diffusion of Ni into the Fe, as observed by Wang *et al.*² This could also be seen in the x-ray absorption spectra, where the peak-to-background ratio decreases upon annealing. This is due to the fact that the absorption cross section at 850 eV (just before the Ni L_3 edge) for Fe is about 5 times higher than for Ni. Figure 2 shows the total absorption spectra for the 15 ML Ni/Fe sample, as deposited and after the longest annealing. Upon annealing, there is a clear shift of the peaks

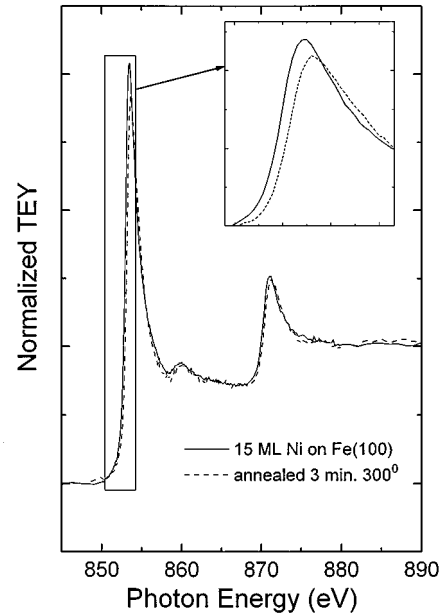


FIG. 2. Ni $L_{2,3}$ absorption edges for 15 ML of Ni on Fe(001), as deposited and after annealing at 300 °C for 3 min. The shift, better shown in the inset, is about 200 meV.

to higher photon energy, of about 150–200 meV. This is in agreement with the shift of the $2p_{3/2}$ and $2p_{1/2}$ core levels with respect to Ni metal found in x-ray photoelectron spectroscopy (XPS) for many Ni alloys.^{20,21} For a dilute alloy of an element Z (in this case Ni) in a host A (Fe), one expects a chemical shift of the levels of element Z if the heats of solution of the Z and $Z+1$ (Cu) elements in A are different.²² The observation of the LEED pattern of the Fe bcc substrate, the decreasing ratio of the Ni to Fe MVV lines in the Auger spectra and the energy shift in XAS, together strongly suggest that Ni is forming a bcc alloy with Fe. The phase diagram of Ni/Fe gives a bulk bcc phase for up to 10% Ni in Fe,²³ but the presence of a bulk substrate might stabilize the bcc structure for the Ni/Fe alloy layers also for higher Ni contents. In Fig. 3, only the L_3 part of the spectra of Fig. 2 is shown, together with the spectra for the flashed and shortly annealed layer. The spectra were aligned to the same edge position, to better show the relative changes in line shape. Also reported is the difference between the spectra for the as-deposited layer and after the last annealing. There is a considerable change in the line shape: the white line intensity is seen to go down, while the intensity of the satellite at ~ 6 eV from the main peak stays more or less constant. In Fig. 4(a), the total absorption spectrum for a thin layer of Ni, annealed for 1 min at 400 °C immediately after evaporating, is compared with the spectrum of Ni metal. The satellite gets significantly broader, comparable to what was observed for the epitaxial layers. After annealing this very thin layer, Ni can be considered as an impurity in the bcc iron, so that both the structure and the type of neighbors have changed with respect to the fcc Ni metal. In Fig. 4(b), the XMCD curves of the spectra in Fig. 4(a) are reported.

To derive the orbital and spin moments for the annealed samples, the same procedure was used as for the as-deposited layers, and the results are listed in Table I. After annealing, the spin moments for all the samples are more or less equal,

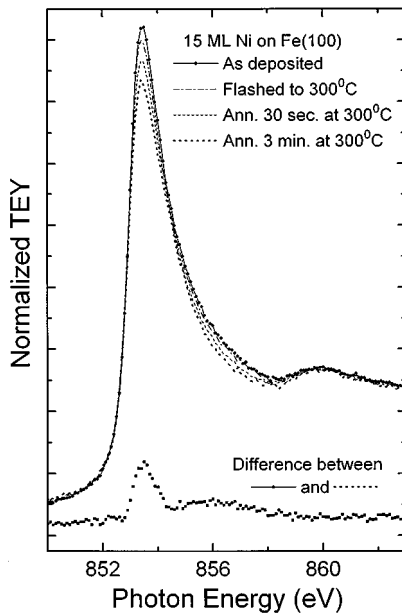


FIG. 3. L_3 edges for 15 ML of Ni on Fe(001), as deposited and after heat treatment. The spectra are shifted to the same edge position, with shifts of 20, 110, and 200 meV for the three subsequent annealings. Also shown is the difference between the spectra for the as-deposited layer and after the longest annealing.

but the orbital moments increase with decreasing thickness of the deposited layer. For the Ni in the annealed 1 ML sample, which in the rest of this paper we will refer to as “Ni impurity,” it is almost twice as large as for bulk Ni. The value obtained for the total moment of the impurity ($0.63\mu_B$) is slightly smaller than theoretical values^{24–26} for Ni in bcc Fe ($0.7–0.79\mu_B$). However, the theoretical moment depends quite strongly on the local Fe structure around Ni since for Ni impurities in fcc Fe or amorphous Fe values of $0.56\mu_B$ (Ref. 24), respectively $0.48\mu_B$ (Ref. 26) are reported.

IV. DISCUSSION

The most striking changes upon alloying Ni with Fe are the decrease of the white line intensity and the strong increase of the orbital moment. In this section, a tentative interpretation of these results will be given.

A. Line shapes

The $L_{2,3}$ absorption spectrum of Ni has been explained in both the itinerant and localized models. In the former, the white lines are the result of transitions from the $2p^63d^9$ ground state to $2p^53d^{10}$ final states (with $2p_{3/2}$ and $2p_{1/2}$ core hole). The satellite at 6 eV above the white lines (hardly visible for the L_2 edge) emerges from the band structure²⁷ and can be attributed to states of d character hybridized with the unoccupied sp band. Upon alloying with Fe, not only the nature of the nearest neighbors changes (from Ni to Fe), but also the structure (from fcc to bcc) and thus the number of nearest neighbors (from 12 to 8). This will influence the band structure and, in turn, also the absorption spectrum. In x-ray photoelectron spectroscopy (XPS) studies of the core levels and valence bands of a large number of alloys, Fuggle *et al.*^{20,21} found that upon alloying of Ni with more electropositive elements the density of d states of Ni at the Fermi level decreases, indicating a filling of the d band. This is in agreement with the decrease of the white line intensity found in the present experiment, where Ni is slightly more electronegative than Fe [the Pauling negativity is 1.9 for Ni and 1.8 for Fe (Ref. 28)]. Fuggle *et al.*²⁰ also suggested that the d state density in the unoccupied sp band is spread out upon alloying, which would be consistent with the broadening of the satellite observed here [Fig. 4(a)].

In the localized model [or many-body configuration interaction (CI) approach] the ground state of Ni is described as a superposition of d^8v^2 , d^9v^1 , and d^{10} configurations, where v^1 and v^2 mean that there is one, respectively two, extra electron(s) in the “reservoir,” in Ni metal mainly consisting of neighboring Ni $3d$ orbitals.^{29–31} In this model the satellite can be caused both by mixing between the $2p^53d^9$ and

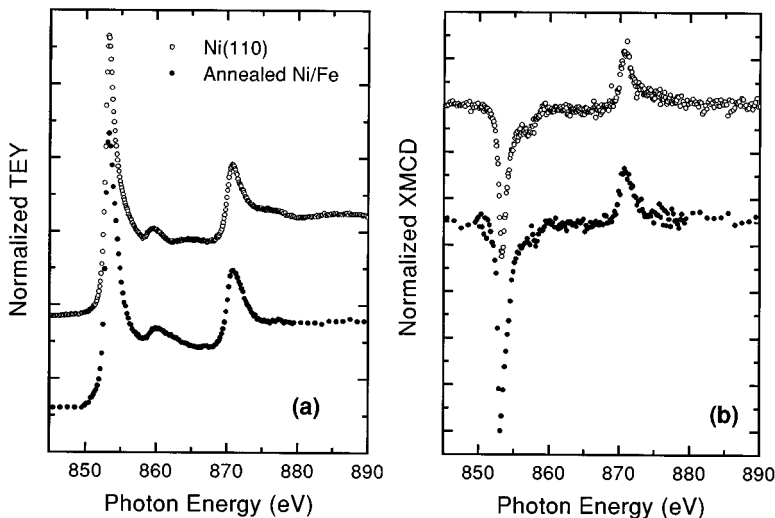


FIG. 4. Total absorption (a) and XMCD (b) for 1 ML of Ni on Fe(001), after annealing (●), compared to bulk fcc Ni (○). The spectrum for Ni on Fe has been corrected for the Fe background.

$2p^53d^{10}$ configurations in the final states and by $3d^8$ character in the ground state.²⁹ This last contribution to the spectrum consists of a multiplet, of which the 3F term is the lowest lying in energy. Since this is a triplet state, with two holes with equal spin, it is expected to play an important role in the magnetism of Ni.^{32,33} It is also responsible, within this model, for the shoulder observed in the XMCD curve of Ni (Ref. 34). The number of parameters in the CI model makes it quite difficult to attribute changes in the experimental spectrum to one mechanism. The strength of the satellite in this model depends critically on the hybridization between the d^8 and d^9 configurations in the ground state (and their energy difference Δ) and on the hybridization between the $2p^53d^9$ and $2p^53d^{10}$ configurations in the final state (see for instance Refs. 35 and 36). Δ is the charge transfer energy, i.e., the energy cost to transfer a hole from a Ni atom to a neighboring atom [$\Delta = E(d^{10}) + E(d^9v) - 2E(d^9)$]. Upon alloying with Fe the character of the “reservoir” states changes and therefore also the relative energy and occupation of the d^8v^2 , d^9v^1 , and d^{10} configurations. The relative intensity of the 4 eV shoulder in the XMCD curve is lower for the Ni impurity than for the Ni metal [see Fig. 4(b)]. Also in the difference between the total absorption spectra (Fig. 3) a shoulder is observed at the same position as in the XMCD curve. This indicates a decrease in the amount of d^8 character in the ground state, which is consistent with a filling of the d band.

In conclusion, the shift of the Ni absorption spectrum upon alloying, the lowering of the white line intensity, and the broadening of the satellite agree well with previous results obtained using XPS.^{20,21} Like the decrease in the ratio of the satellite to the main line in the XMCD curve, they can be attributed to the filling of the Ni d band. However, we do not see an obvious explanation for the increase in ratio between the intensities of the satellite and the white line in the total absorption spectrum.

B. Magnetic moments

In atoms, the size of the orbital magnetic moment is dictated by the electron-electron interaction (the first two Hund’s rules). In the solid state other parameters influence the orbital moment as well, like the symmetry and the strength of the crystal field, the spin-orbit coupling, the size of the spin moment and the density of states at the Fermi level. We will try to examine how they relate to the increase of the orbital magnetic moment observed in Ni/Fe bcc alloys.

From Table I, it can be seen that there is no difference in the spin moments for Ni metal and the Ni impurity, so this factor can not be very important. The difference in structure between Ni metal fcc and the Ni impurity (bcc) does not change the symmetry of the crystal field (O_h in both cases), but the character of the states at the Fermi level changes, as well as the number of nearest neighbors (from 12 for fcc to 8 for bcc). However, Table I shows that for the 15 ML of Ni after annealing the orbital moment is still more or less equal to that of the Ni metal, though the observed LEED pattern is already close to the one of the clean Fe bcc substrate, suggesting a bcc structure for the Ni as well. The change in structure apparently does not have much influence on the size of the orbital moment.

Apart from changing the structure, annealing also causes intermixing, resulting in replacement of part of the Ni neighbors by Fe. After annealing the thinnest layer, the Ni atoms will have almost only Fe neighbors. It could, therefore, be the *nature* of the nearest neighbors which gives rise to the increase of the orbital moment. This would also explain the trend in the orbital moment with the thickness of the deposited layers. For the thicker layers the Ni concentration after annealing will strongly depend on the depth, and close to the surface the number of Ni-Ni bonds will still be considerable, especially for the 15 ML sample.

At a first glance, the increase of the orbital moment agrees well with calculations of Söderlind *et al.*³⁷ for Fe-Co and Co-Ni alloys. In these calculations, the spin-up band is essentially filled and the rigid spin-down band gets gradually filled going from Fe, via Co, to Ni, supposing “average” atoms with an atomic number which is the concentration weighted atomic number of the alloy. They show a strong increase of the orbital magnetic moment going from Ni to a bcc alloy at 25% Ni in Co. The maximum of the orbital moment is related to a high spin-down DOS at the Fermi energy around that composition. XMCD results by Idzerda *et al.*³⁸ show, however, a similar increase in the orbital to spin moment ratio for diluted Fe in Co and Co in Fe, which cannot be explained by the above mentioned theory. The calculations of Söderlind *et al.*³⁷ also suppose an emptying of the d band going from Ni to Co, while the opposite is observed upon alloying with Fe. Our results, together with those of Idzerda *et al.*,³⁸ suggest that the increase of the orbital moment is inherent to the impurity character of the absorber. One of the reasons has already been mentioned: the strength of the crystal field, as well as the hybridization, depends on the amount of covalency between the atoms, and this will always decrease when, in a certain structure, the nearest neighbors are changed from equivalent atoms to those of another element. The electronic states of an impurity are more localized on the impurity atom site, which increases the electron-electron interaction and the spin-orbit coupling, and therefore decreases the quenching of the orbital moment. A higher localization of the electron states is also expected at the surface, an argument which was recently used to explain the increased orbital moment found at the surface of Ni metal³⁹ and for thin Co layers on Cu (Ref. 40).

V. CONCLUSIONS

We have used absorption spectroscopy with polarized x rays to investigate the magnetic properties of Ni layers deposited on an Fe(001) crystal. The main results and information drawn from the experiment can be summarized as follows.

We have not observed any linear dichroism, within our experimental sensitivity, in thin (1–3 ML) bcc layers of Ni on Fe. Since linear dichroism measures the expectation value of $Q_{zz} = [3J_z^2 - J(J+1)]$ (Ref. 18), which in turn is the main source¹⁷ of dipolar momentum $\langle T_z \rangle$ for Ni, we conclude that $\langle T_z \rangle$ is small for our bcc Ni layers. This result allows a more confident use of the simplified sum rule for the spin moment applied to circular dichroism data, and supports our previous analysis.⁷

For 5–15 ML thick Ni layers, we have used the sum rules

to obtain magnetic moments from circular dichroism data. We have found values, along the magnetization direction of the substrate, of $0.3 \pm 0.1 \mu_B$, without apparent dependence on the layer thickness.

For a Ni impurity in Fe, obtained by annealing a thin (1 ML) layer of Ni on Fe(001), we have obtained a Ni spin moment ($0.26 \mu_B$) close to the one of fcc Ni ($0.27 \mu_B$), but an orbital moment of $0.11 \mu_B$ which is almost twice the one found in the bulk ($0.06 \mu_B$).

Our results indicate that neither the specific structure and coordination (bcc, 8 neighbors), nor the size of the spin moment are of major importance to interpret the increase of the

orbital moment. The "impurity" character of Ni diluted in Fe might well, on the contrary, explain our findings, through a stronger localization of the d orbitals on the Ni site and a consequently reduced quenching of the orbital moment.

ACKNOWLEDGMENT

This work has been supported in part by the stichting Scheikundig Onderzoek in Nederland (SON) with financial support from the Nederlandse organisatie voor Wetenschappelijk Onderzoek (NWO), and by the European Community under Contract No. SC1-CT91-0630.

-
- *Present address: Laboratoire de Magnétisme Louis Néel, Centre National de la Recherche Scientifique, 166X, 38042 Grenoble CEDEX, France.
- ¹B. Dieny, *J. Magn. Magn. Mater.* **136**, 335 (1994), and references therein.
 - ²Z. Q. Wang, Y. S. Li, F. Jona, and P. M. Marcus, *Solid State Commun.* **61**, 623 (1987).
 - ³B. Heinrich, S. T. Purcell, J. R. Dutcher, K. B. Urquhart, J. F. Cochran, and A. S. Arrott, *Phys. Rev. B* **38**, 12 879 (1988).
 - ⁴M. D. Wiczorek, D. J. Keavney, D. F. Storm, and J. C. Walker, *J. Magn. Magn. Mater.* **121**, 34 (1993).
 - ⁵V. L. Moruzzi, P. M. Marcus, K. Schwarz, and P. Mohn, *Phys. Rev. B* **34**, 1784 (1986).
 - ⁶J. I. Lee, S. C. Hong, A. J. Freeman, and C. L. Fu, *Phys. Rev. B* **47**, 810 (1993).
 - ⁷J. Vogel, G. Panaccione, and M. Sacchi, *Phys. Rev. B* **50**, 7157 (1994).
 - ⁸Ph. Sainctavit, D. Lefebvre, Ch. Cartier dit Moulin, C. Lafon, Ch. Brouder, G. Krill, J.-Ph. Schillé, J.-P. Kappler, and J. Goulon, *J. Appl. Phys.* **72**, 1985 (1992); D. Lefebvre, Ph. Sainctavit, and C. Malgrange, *Rev. Sci. Instrum.* **65**, 2556 (1994).
 - ⁹J. Vogel and M. Sacchi, *Phys. Rev. B* **49**, 3230 (1994).
 - ¹⁰W. O'Brien and B. L. Tonner, *Phys. Rev. B* **50**, 12 672 (1994).
 - ¹¹B. T. Thole, P. Carra, F. Sette, and G. van der Laan, *Phys. Rev. Lett.* **61**, 1943 (1992).
 - ¹²P. Carra, B. T. Thole, M. Altarelli, and X.-D. Wang, *Phys. Rev. Lett.* **70**, 694 (1993).
 - ¹³R. Wu, D. Wang, and A. J. Freeman, *Phys. Rev. Lett.* **71**, 3581 (1993); *J. Magn. Magn. Mater.* **132**, 103 (1994).
 - ¹⁴C. T. Chen, Y. U. Idzerda, H.-J. Lin, N. V. Smith, G. Meigs, E. Chaban, G. H. Ho, E. Pellegrin, and F. Sette, *Phys. Rev. Lett.* **75**, 152 (1995).
 - ¹⁵G. Y. Guo, H. Ebert, W. T. Temmerman, and P. J. Durham, in *Metallic Alloys: Experimental and Theoretical Perspectives*, edited by J. S. Faulkner (Kluwer Academic, Dordrecht, 1993).
 - ¹⁶R. Wu and A. J. Freeman, *Phys. Rev. Lett.* **73**, 1994 (1994); R. Wu, D. Wang, and A. J. Freeman, *J. Magn. Magn. Mater.* **132**, 103 (1994).
 - ¹⁷B. T. Thole (private communication).
 - ¹⁸P. Carra, H. König, B. T. Thole, and M. Altarelli, *Physica B* **192**, 182 (1993).
 - ¹⁹G. Y. Guo, H. Ebert, W. M. Temmerman, and P. J. Durham, *Phys. Rev. B* **50**, 3861 (1994).
 - ²⁰J. C. Fuggle, F. U. Hillebrecht, R. Zeller, Z. Zolnieriek, P. Bennet, and Ch. Freiburg, *Phys. Rev. B* **27**, 2145 (1982).
 - ²¹F. U. Hillebrecht, J. C. Fuggle, P. A. Bennet, Z. Zolnieriek, and Ch. Freiburg, *Phys. Rev. B* **27**, 2179 (1982).
 - ²²P. Steiner, S. Hüfner, N. Mårtensson, and B. Johansson, *Solid State Commun.* **37**, 73 (1981); P. Steiner and S. Hüfner, *ibid.* **37**, 79 (1981).
 - ²³M. Hansen, *Constitution of Binary Alloys* (McGraw-Hill, New York, 1958).
 - ²⁴V. I. Anisimov, V. P. Antropov, A. I. Liechtenstein, V. A. Gubanov, and A. V. Postnikov, *Phys. Rev. B* **37**, 5598 (1988).
 - ²⁵B. Drittler, N. Stefanou, S. Blügel, R. Zeller, and P. H. Dederichs, *Phys. Rev. B* **40**, 8203 (1989).
 - ²⁶O. Yu. Kontsevoi and V. A. Gubanov, *Phys. Rev. B* **51**, 15 125 (1995).
 - ²⁷N. V. Smith, C. T. Chen, F. Sette, and L. F. Mattheis, *Phys. Rev. B* **46**, 1023 (1992).
 - ²⁸L. Pauling, *The Nature of the Chemical Bond* (Cornell University Press, Ithaca, NY, 1960).
 - ²⁹T. Jo and G. A. Sawatzky, *Phys. Rev. B* **43**, 8771 (1991).
 - ³⁰G. van der Laan and B. T. Thole, *J. Phys. Condens. Matter* **4**, 4181 (1992).
 - ³¹A. Tanaka and T. Jo, *J. Phys. Soc. Jpn.* **61**, 2669 (1992).
 - ³²J. C. Fuggle, P. Bennet, F. U. Hillebrecht, A. Lenselink, and G. A. Sawatzky, *Phys. Rev. Lett.* **49**, 1787 (1982).
 - ³³P. A. Bennet, J. C. Fuggle, F. U. Hillebrecht, A. Lenselink, and G. A. Sawatzky, *Phys. Rev. B* **27**, 2194 (1982).
 - ³⁴C. T. Chen, F. Sette, Y. Ma, and S. Modesti, *Phys. Rev. B* **42**, 7262 (1990).
 - ³⁵J. Zaanen, in *Unoccupied Electronic States*, edited by J. C. Fuggle and J. E. Inglesfield (Springer-Verlag, Berlin, 1992).
 - ³⁶F. M. F. de Groot, Ph.D. thesis, University of Nijmegen, 1991.
 - ³⁷P. Söderlind, O. Eriksson, B. Johansson, R. C. Albers, and A. M. Boring, *Phys. Rev. B* **45**, 12 911 (1992).
 - ³⁸Y. U. Idzerda, C. J. Gutierrez, L. H. Tjeng, H.-J. Lin, G. Meigs, and C. T. Chen, *J. Magn. Magn. Mater.* **127**, 109 (1993).
 - ³⁹G. van der Laan, M. A. Hoyland, M. Surman, C. F. J. Flipse, and B. T. Thole, *Phys. Rev. Lett.* **69**, 3827 (1992).
 - ⁴⁰M. Tischer, O. Hjortstam, D. Arvanitis, J. Hunter Dunn, F. May, K. Baberschke, J. Trygg, J. M. Wills, B. Johansson, and O. Eriksson, *Phys. Rev. Lett.* **75**, 1602 (1995).